Process for the Formation of Biaxially Oriented Films of Poly(*p*-phenylene Terephthalamide) from Liquid Crystalline Solutions

JOHN E. FLOOD, JAMES L. WHITE, and JOHN F. FELLERS,
Polymer Engineering, University of Tennessee, Knoxville, Tennessee 37996

Synopsis

A new process for making equal biaxially oriented films from liquid crystalline solutions of poly(p-phenylene terephthalamide) (PPD-T) is described. The process involves extruding solutions of PPD-T/H_2SO_4 through an annular die and over an oil-coated mandrel into a coagulation bath. The films were studied using wide angle X-ray diffraction (WAXS) and scanning electron microscopy (SEM). Tensile stress–strain properties were obtained on samples cut at various directions in the plane of the film. Biaxially oriented films which possess equal properties in the various directions in the plane of the film were produced. Moduli of 2.3×10^9 Pa and tensile strengths of 9.6×10^7 Pa were obtained in the plane of the film. Films with unequal biaxial orientation were also produced. These tend to have higher modulus/tensile strength in the direction of major orientation, the machine direction (up to 8.3×10^9 Pa/2.5×10^8 Pa), but become brittle in the transverse direction.

INTRODUCTION

One of the most striking developments in polymer technology during the past decade has been duPont's development of high modulus and tensile strength aromatic polyamide fibers through the spinning of liquid crystalline polymer solutions.[1–4] This technology, largely reproduced some years ago in our own[5] and other industrial laboratories,[6] has inspired various research teams to both search for new liquid crystalline polymer systems[7–18] and investigate their structure in the quiescent state[14,17,19,20] and in flow.[16,21–25] This has, in turn, led to continuing efforts in various industrial concerns[7–11,15] and our own laboratories[16,26] to develop new fiber spinning processes based on a range of liquid crystalline polymer fluids.

As indicated in the above paragraph, the industrial processing efforts have been almost entirely involved in the development of high modulus fibers. Only two research teams have described efforts to develop more complex processing procedures and products. Tennessee Eastman investigators[8,9] have described the injection molding of liquid crystalline polyesters. The second process is one developed in our own laboratories which involves the continuous formation of film from solutions of poly(p-phenylene terephthalamide) (PPD-T) or redissolved Kevlar® fiber in sulfuric acid. Aoki et al.[27] have described a process in which solution emerging from an annular die is extruded and internally pressured with gas, analogous to tubular film extrusion. The blown PPD-T/H_2SO_4 fluid annulus then entered a water bath which extracted the H_2SO_4 and coagulated the PPD-T. It was not, however, possible to develop a high level of biaxial orientation in this manner, and the process did not operate in a stable manner.

It is our purpose in the present paper to describe an improved process for

Journal of Applied Polymer Science, Vol. 27, 2965–2985 (1982)
 CCC 0021-8995/82/082965-21$03.10

producing PPD-T films. The new process involves the use of extrusion from an annular die over an external mandrel rather than a tubular blowing procedure. Mandrel processes have a long history in polymer processing. More than a century ago Hyatt[28] developed and applied such a technique to produce hollow shapes from Celluloid. There have been in latter years various patents using mandrel processes for producing tubing, sheeting, and film,[29–34] though none has dealt with liquid crystalline polymers or PPD-T.

MATERIALS

The starting polymer was duPont Kevlar® 29 which has been identified by various investigators as being poly(p-phenylene terephthalamide) (PPD-T):

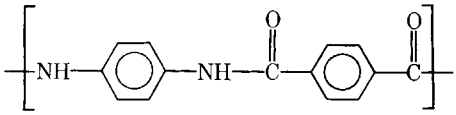

(1)

This was dissolved in 100% sulfuric acid prepared by mixing together fuming sulfuric acid (with 30% excess SO_3 obtained from Fisher Chemical) with 96% concentrated sulfuric acid (also from Fisher Chemical).

The dissolution of Kevlar® 29 in sulfuric acid was carried out in a dry box filled with nitrogen to avoid absorption of moisture. Mixing was first carried out by hand at about 60–70°C. This is followed by periods of "shaking" in a mechanical blender. The mixing step involves combining typically 350–375 mL of H_2SO_4 with 120–130 g of Kevlar in an 800-mL jar. Bubbles are removed from the polymer solutions by means of a vacuum pump.[35]

MANDREL FILM PROCESS

Description

The film was produced by extrusion through an annular die using the apparatus of Figures 1–3. Oil is fed through a 0.25-hp Zenith gear pump into a cylindrical reservoir containing a piston below which is the solution of PPD-T/H_2SO_4. The oil pressure forces the piston downward, pushing the solution into an annular die of inside radius 49.45 mm and annular gap of 0.3 mm. The reservoir and annular die system are made for Type 304 stainless steel to prevent corrosion by the H_2SO_4. The piston is made from stainless steel surrounded by a Teflon® seal.

The solution emerges from the die and flows or is drawn over a conical mandrel made from poly(vinyl chloride). The mandrel is coated with an oil pumped from an overhead separatory funnel through the die. The purpose of the oil is to reduce friction and induce biaxial elongational flow in the PPD-T/H_2SO_4 solution. The mandrel used is 107 mm high, with a diameter of 33 mm at its top and 165 mm at its bottom.

The film moves from the mandrel into the coagulation bath at room temperature which contains liquids such as water, methanol (MeOH), ethanol (EtOH), or their mixtures. These liquids extract the H_2SO_4 from the solution and

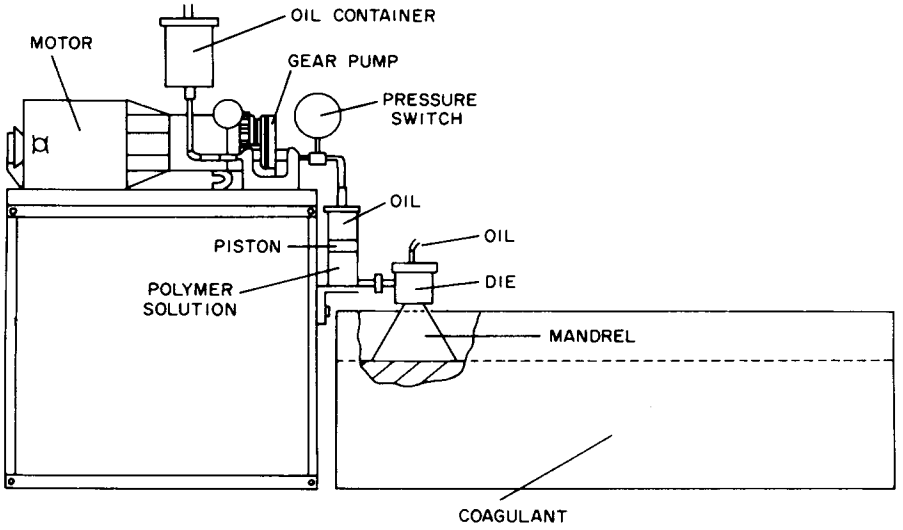

Fig. 1. Schematic of PPD-T/H_2SO_4 film forming process with mandrel.

coagulate the PPD-T into a film. The film is taken up at the other end of the bath. More detailed information on apparatus design is given by Flood[35] elsewhere.

Process Analysis

Let us take the flow direction to be "1", the transverse direction around the circumference of mandrel to be "2" and the thickness direction to be "3". Our process involves the two phase flow of a PPD-T solution and an oil over a conical mandrel. We need first concern ourselves with the velocity profiles in the two phases. Taking the thickness H of the solution plus the oil layers to be much less than the radius of curvature of the mandrel, we may presume the flow to be equivalent to approximately gravity flow down an inclined plane. This is described by a force balance relating gravity forces and shear stress σ_{13} according to[36]

$$\frac{d\sigma_{13}}{dx_3} = -\rho_j g \cos\theta \tag{1}$$

where θ is the half-cone angle and ρ_j is the density of the j phase. If we presume each of the phases a Newtonian fluid and neglect the differences in their densities, the velocities of the oil and solution phases are simply

$$(v_1)_{oil}(x_3) = \frac{\rho g \cos\theta}{2\eta_{oil}}[2Hx_3 - x_3^2] \tag{2a}$$

$$(v_1)_{sol}(x_3) = \frac{\rho g \cos\theta}{2\eta_{sol}}\left[\left(1 - \frac{\eta_{oil}}{\eta_{sol}}\right)(2H\Delta - \Delta^2) + \frac{\eta_{oil}}{\eta_{sol}}(2Hx_3 - x_3^2)\right] \tag{2b}$$

If the viscosity of the solution is much greater than that of the oil, the velocity profile in the solution goes to

$$(v_1)_{sol} = \frac{\rho g \cos\theta}{2\eta_{sol}}[2H\Delta - \Delta^2] \tag{3}$$

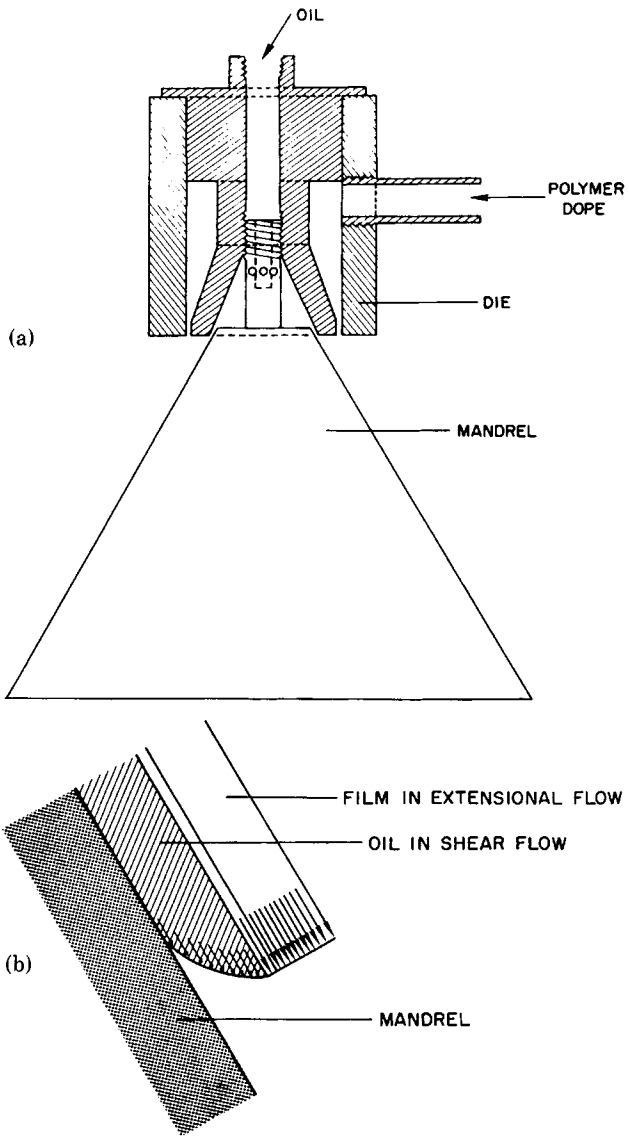

Fig. 2. (a) Detail of die and mandrel; (b) film in extensional flow over oil lubricated mandrel.

The velocity field becomes plug flow. This means that the flow field is purely elongational.

The conclusions of the above paragraph should remain valid if the fluid is non-Newtonian with a viscosity decreasing as a function of shear rate. Indeed the tendency to a flat velocity profile is even accentuated by this effect.

We presume elongational flow in the PPD-T/H_2SO_4 film moving down the mandrel. Letting h be the thickness of the solution film and R the local cone radius, the velocity gradients in the film are[37,38]

$$\frac{\partial v_3}{\partial \xi_3} = \frac{Q \cos\theta}{2\pi R h}\left(\frac{1}{h}\frac{dh}{dz}\right) \tag{3a}$$

(a)

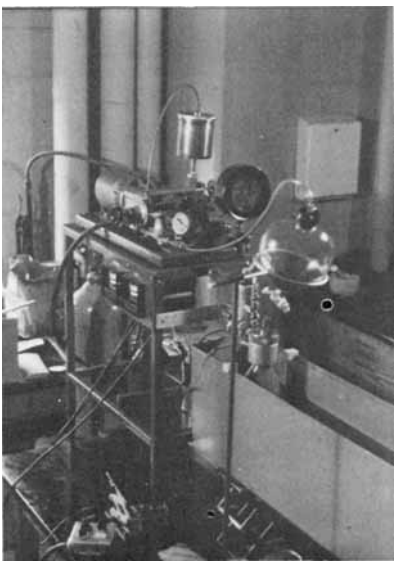

(b)

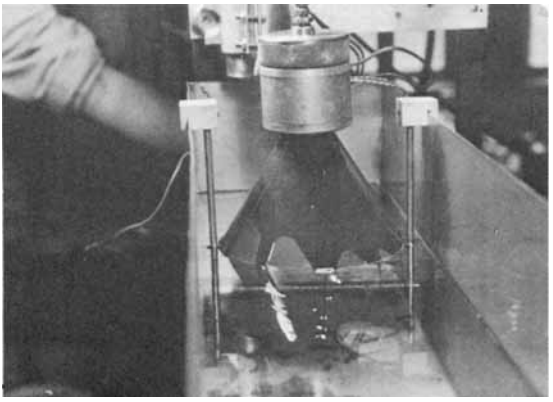

Fig. 3. Photographs of equipment and its operation: (a) overview; (b) coating of mandrel with oil; (c) emergence of PPD-T/H_2SO_4 solution over oil-coated mandrel; (d) normal operation of process with PPD-T/H_2SO_4 and oil-coated mandrel.

$$\frac{\partial v_2}{\partial \xi_2} = \frac{Q \cos\theta}{2\pi Rh}\left(\frac{1}{R}\frac{dR}{dz}\right) \tag{3b}$$

$$\frac{\partial v_1}{\partial \xi_1} = \frac{Q \cos\theta}{2\pi Rh}\left(-\frac{1}{h}\frac{dh}{dz} - \frac{1}{h}\frac{dR}{dz}\right) \tag{3c}$$

Here Q is the extrusion rate and z the altitude of the cone. The expanding radius $R(z)$ of the cone ensures a velocity gradient in the transverse direction.

Various special cases may be noted. If we consider takeup of the annular film in the absence of the mandrel, uniaxial extension results,

$$\frac{\partial v_2}{\partial \xi_2} = \frac{\partial v_3}{\partial \xi_3} \tag{4a}$$

Thus

$$\frac{1}{R}\frac{dR}{dz} = \frac{1}{h}\frac{dh}{dz} \tag{4b}$$

(c)

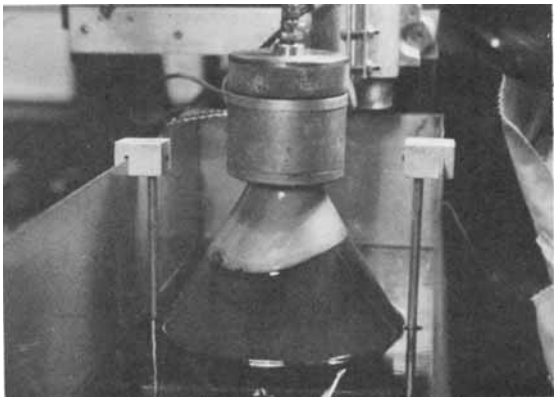

(d)

Fig. 3. (*Continued from previous page.*)

which leads to the emerging annulus being drawn down through the air gap according to

$$\frac{R(z)}{R_0} = \frac{h(z)}{h} = \left[\frac{v_1(0)}{v_1(z)}\right]^{1/2} \tag{4c}$$

If the mandrel is present, $R(z)$ must be an increasing function defined by the mandrel shape. We desire an equal biaxial extension. For this case

$$\frac{\partial v_1}{\partial \xi_1} = \frac{\partial v_2}{\partial \xi_2} \tag{5a}$$

Thus

$$-\frac{1}{R}\frac{dR}{dz} - \frac{1}{h}\frac{dh}{dz} = \frac{1}{R}\frac{dR}{dz} \tag{5b}$$

which leads to

$$\frac{R(z)}{R_0} = \left(\frac{h_0}{h(z)}\right)^{1/2} = \frac{v_1(z)}{v_1(0)} \tag{5c}$$

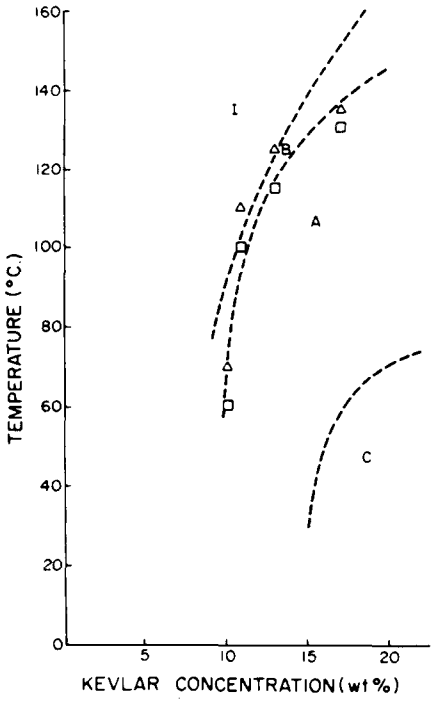

Fig. 4. Approximate phase diagram of PPD-T/H_2SO_4, indicating concentration temperature-dependence of liquid crystalline regions: (I) isotropic; (B) biaphasic; (A) anisotropic; (C) solid crystalline. Data points: (△) onset of I → A transition; (□) completion of I → A transition.

Such a case is possible in the presence of a mandrel. However, to achieve this, the fluid must also respond in a manner compatible with the balance of forces.

Equilibrium of forces in flow down a mandrel derive from the theory of membranes.[39] These have the form

$$\frac{d}{d\theta} Rh\sigma_{11} - r_a h\sigma_{22} \cos\theta + p_\theta R r_a = 0 \tag{6a}$$

$$\frac{h\sigma_{11}}{r_a} + \frac{h\sigma_{22}}{r_b} = p_r \tag{6b}$$

Here r_a and r_b are radii of curvature in the machine and transverse directions (see Fig. 1). p_r and p_θ are related to the pressures within the oil and gravity through

$$p_r = p - \rho g h \cos\theta \tag{7a}$$

$$p_\theta = \rho g h \sin\theta \tag{7b}$$

where p is ambient (atmospheric) pressure.

The stress σ_{11} may be shown to be of form

$$\sigma_{11} = \frac{1}{rh \sin\theta} [\int r_a r_b (p_r \cos\theta - p_\theta \sin\theta) \sin\theta \, d\theta + C] \tag{8}$$

where C is a constant of integration.

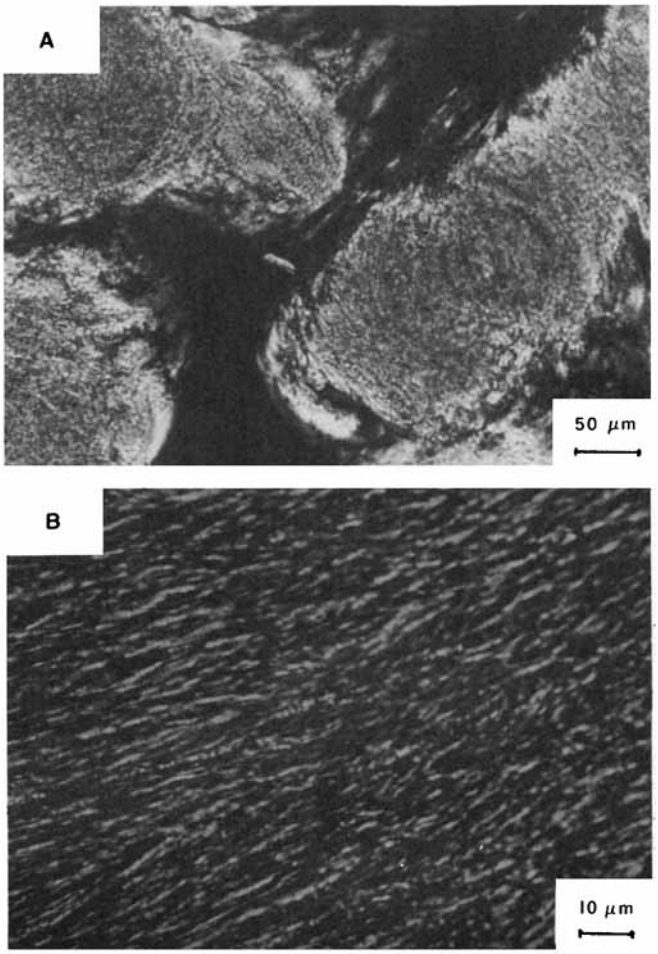

Fig. 5. Polarized light photomicrographs of liquid crystalline PPD-T/H_2SO_4 solutions: (A) 12% PPD-T at 70°C; (B) 17% PPD-T at 70°C.

To proceed further, we need a constitutive equation describing the flow characteristics of the solution. Such formulations do not exist for liquid crystalline polymer systems. However, this type of problem has been investigated for both Newtonian fluid[40] and elastic solid[41,42] models.

Process Conditions

It is possible to operate the apparatus over a wide range of conditions of concentrations and temperatures, especially without the mandrel. The conditions where the mandrel is required are more limited but still broad. It was, however, our intention to operate under conditions wherein the PPD-T/H_2SO_4 solutions are in a liquid crystalline form. This is defined by the approximate phase diagram of Figure 4, which shows the concentration and temperature conditions under this system exists in different forms. This figure was constructed from both observations using a Leitz–Wetzlar polarized light microscope and reference to the literature.[1,43] We primarily limited our efforts to liquid crystalline regions.

TABLE I
Process Conditions for Formation of PPD-T Films

Run no.	Coagulant by volume	Blowup ratio	Film process	Temp (°C)	Extrusion rate (mL/min)	Concn (wt %)	Sample thickness (mm)
1	50% MeOH 50% EtOH	1	Extruded	70	85	17	0.9
2	55% MeOH 45% H_2O	1	Extruded	70	85	17	0.7
3	75% MeOH 25% H_2O	1	Extruded	70	85	17	0.99
4	100% H_2O	1	Extruded	70	85	17	0.92
5	50% MeOH 50% EtOH	<1	Drawdown	70	85	17	0.06
6	55% MeOH 45% H_2O	<1	Drawdown	70	85	17	0.026
7	75% MeOH 25% H_2O	<1	Drawdown	70	85	17	0.08
8	100% H_2O	<1	Drawdown	70	85	17	0.04
9	50% MeOH 50% EtOH	3.3	Mandrel	70	85	17	0.012
10	50% MeOH 50% EtOH	3.3	Mandrel	70	85	17	0.01
11	75% MeOH 25% H_2O	3.3	Mandrel	70	85	17	0.01
12	75% EtOH 25% H_2O	3.3	Mandrel	70	85	17	0.01
13	50% MeOH 50% EtOH	3.3	Mandrel with drawdown	70	85	17	0.01

Polarized light photomicrographs of some of the liquid crystalline solutions are shown in Figure 5.

The various process conditions investigated are summarized in Table I. It was found that higher solution concentrations made the polymer solution easier to work with in terms of processability. This necessitates moving to higher temperatures. The optimum conditions were found to be 70°C and a concentration of 17 wt%. At higher temperatures, we started to have problems of chemical stability. Concentrations higher than 17% were considerably more difficult to mix into a homogeneous solution.

Various other processing problems are noted here. The viscosity of the oil coating the mandrel proved important. To have stable film flow over the mandrel, a hydrocarbon oil had to be in the viscosity range 170–370 centipoise. While the densities of the two phases were generally close, it is also necessary to choose the oil coating the mandrel to be denser than the coagulant. This is

TABLE II
Primary WAXS Reflections From PPD-T According to Northolt[47]

WAXS reflections	Bragg spacing (Å)	Bragg angle(°)
110	4.326	20.5
200	3.935	22.57
006	2.15	41.97

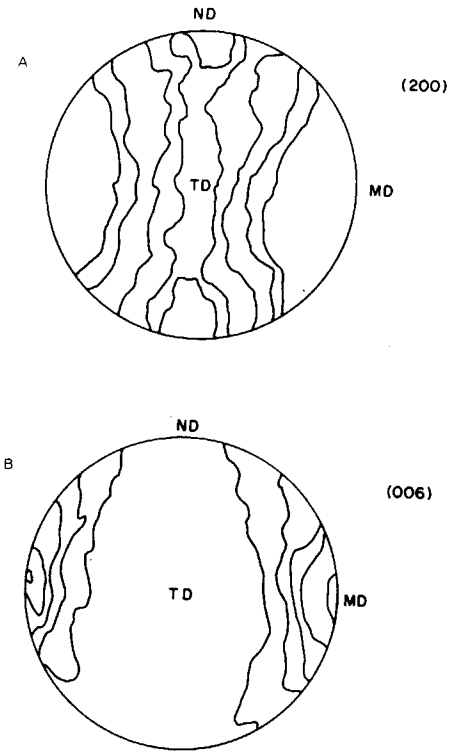

Fig. 6. Pole figures of film extruded through an annular air gap into the coagulation bath: (A) 200 reflection; (B) 006 reflection.

to insure it will sink to the bottom of the tank and not seek to float on the surface. If it floats, it will disrupt the film being formed.

A range of coagulants were used, as may be seen in Table I. Most proved satisfactory from the process point of view. As one proceeds from pure water to pure alcohol, the density decreases. The hydrocarbon oils used with alcohols could not be used with water. In practice we generally used coagulants with 25 wt% or less water.

FILM CHARACTERIZATION

WAXS Measurements

The structure of the films produced were examined using wide angle X-ray diffraction (WAXS). Pole figures[44] were prepared using a single crystal orienter mounted on a General Electric XRD-5 diffractometer. The radiation used was CuKα with a wavelength of 0.154 nm. The films prepared were stacked and glued together at their edges and mounted on the single crystal orienter. This is the same apparatus used in the studies of Choi, Spruiell, and White[45] on polyethylene tubular film.

The biaxial orientation factors of White and Spruiell[38,45,46]

$$f_{1j}^{B} = 2\,\overline{\cos^2\phi_{1j}} + \overline{\cos^2\phi_{2j}} - 1 \tag{7a}$$

$$f_{2j}^{B} = 2\,\overline{\cos^2\phi_{2j}} + \overline{\cos^2\phi_{1j}} - 1 \tag{7b}$$

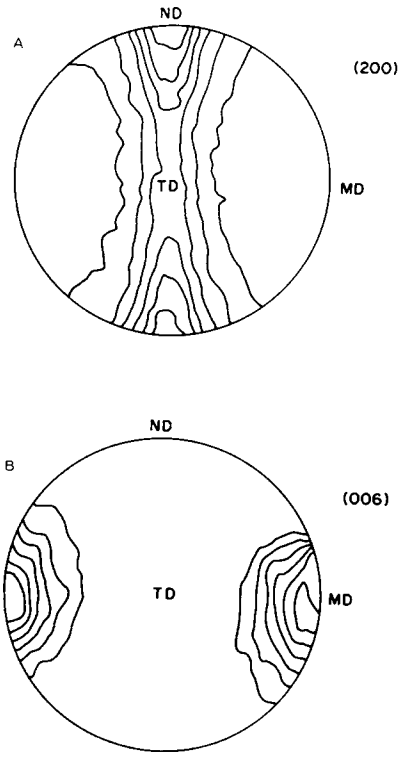

Fig. 7. Pole figures for film extruded through an annular die and then drawn down with a draw-down ratio v_1/v_0: (A) 200 reflection; (B) 006 reflection.

were computed from the pole figures. Here ϕ_{1j} and ϕ_{2j} are the angles between the machine (1) and transverse (2) directions and the j crystallographic axis.

Northolt[47] has reported that an orthorhombic unit cell with unit cell dimensions of $a = 0.787$ nm, $b = 0.518$ nm, $c = 1.29$ nm (chain axis). The primary reflections used were the (110), (200), and (006) (see Table II). The (200) reflection may be used to directly compute $\overline{\cos^2\phi_{1a}}$ and $\overline{\cos^2\phi_{2a}}$. The (200) and (110) reflections were used in the manner of Stein[48] to calculate the $\overline{\cos^2\phi_{1b}}$ and $\overline{\cos^2\phi_{2b}}$. The $\overline{\cos^2\phi_{1c}}$ and $\overline{\cos^2\phi_{2c}}$ were determined from the Pythagorean theorem.

Scanning Electric Microscopy

The films were characterized using an AMR High Resolution Scanning Electron Microscope. The films were coated with a gold-palladium alloy. They were examined along a fracture edge and also normal to the film surface.

Shrinkage

A 5 cm^2 sample was cut from the film while still in the coagulation bath. The film was then placed in the open air for a period of 24 h. Measurements were made to determine the amount of film shrinkage in the machine and the transverse direction.

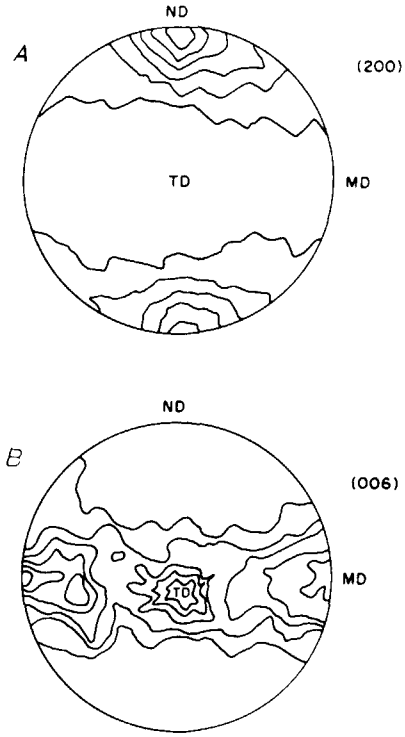

Fig. 8. Pole figures for film extruded through an annular die and over a mandrel into the coagulation bath: (A) 200 reflection; (B) 006 reflection.

Mechanical Properties

Tensile measurements were made on films using a Table Model Instron Tensile Testing Machine. Measurements were made in the machine and transverse directions and at a 45° angle. A gauge length of 20 mm was used in most experiments and the crosshead speed was 2 mm/min.

RESULTS OF FILM CHARACTERIZATION

Thickness

The films produced without drawdown are the thickest, being of order 0.25–1 mm. The films drawn down uniaxially without a mandrel have thickness of order 0.026–0.2 mm. The films drawn over the mandrel are of order 0.005–0.1 mm.

WAXS

WAXS measurements on the films coagulated in alcohol solutions show the reflections described by Northolt[47] and correspond to the orthorhombic unit cell he proposed (see Table II). However, films coagulated in water baths exhibit some different reflections. These are at 0.51 nm, 0.53 nm, and 0.215 nm, respectively.

Typical (006) and (200) pole figures (based on Northolt's unit cell) for a film

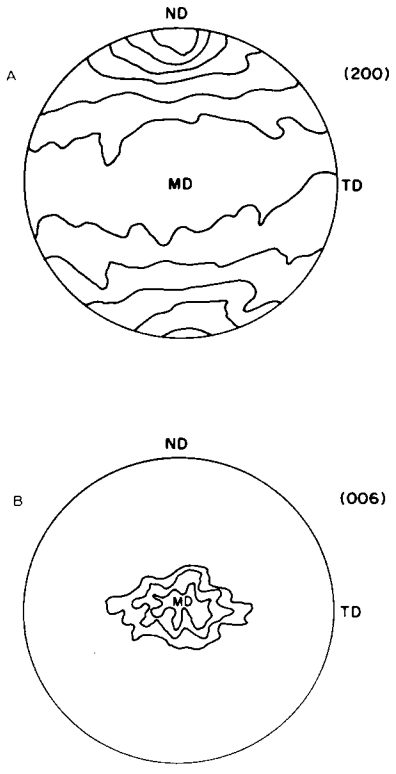

Figure 9. Pole figures for films extruded through an annular die and drawn over a mandrel with higher drawdown ratios: (A) 200 reflection; (B) 006 reflection.

extruded through an annular die into a coagulation bath without takeup are shown in Figure 6. The influence of drawdown on orientation is shown in Figure 7. Introduction of the mandrel makes the orientation of the films vary as shown in Figure 8. The effect of enhanced drawdown over the mandrel is shown in Figure 9.

Figure 6 indicates the existence of uniaxial orientation in the machine direction. The **c**-axis shows some orientation in the machine direction, while the **a**-axis orientation exhibits a symmetric orientation about this axis. Figure 7 shows an enhanced uniaxial orientation.

The film pulled down over the mandrel shows a biaxial orientation with the **c**-axis being approximately equally distributed between the machine direction and the transverse direction. This is shown in Figure 8. Polymer chain orientation in the machine direction is increased as the drawdown is increased (Figure 9).

Biaxial orientation factors were determined from the pole figures. These results are summarized in Table III. Figure 10 uses the orientation triangle of White and Spruiell[46] to represent the c-axis orientation factors. The films extruded directly into the bath may be seen to place near the f_{1c}^{B} axis indicating some uniaxial orientation. They have f_{1c}^{B} of 0.3 and f_{2c}^{B} of 0.1. Films drawn down without a mandrel appear at a higher position on the f_{1c}^{B} axis, indicating much higher uniaxial orientation. They have f_{1c}^{B} about 0.47 and f_{1c}^{B} of 0.13. Stretching

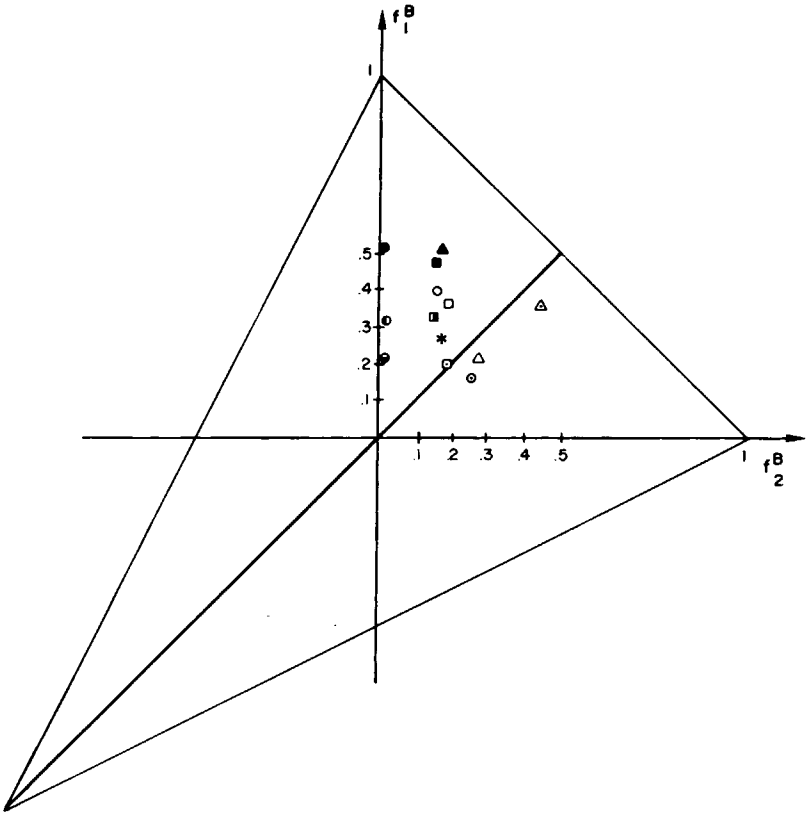

Fig. 10. Orientation triangle for C-axis orientation factors: (◑) 1; (◒) 2; (□) 3; (◨) 4; (●) 5; (▲) 6; (○) 7; (■) 8; (*) 9; (⊡) 10; (⊙) 11; (△) 12; (◬) 13.

the film over a mandrel creates nearly equal biaxial orientation factors placing the data approximately on an altitude of the orientation triangle. Values of f_{1c}^B about 0.25 and f_{2c}^B of 0.28 are obtained. With increasing drawdown ratios, the orientation factors place at an intermediate position between the f_{1c}^B axis and the altitude.

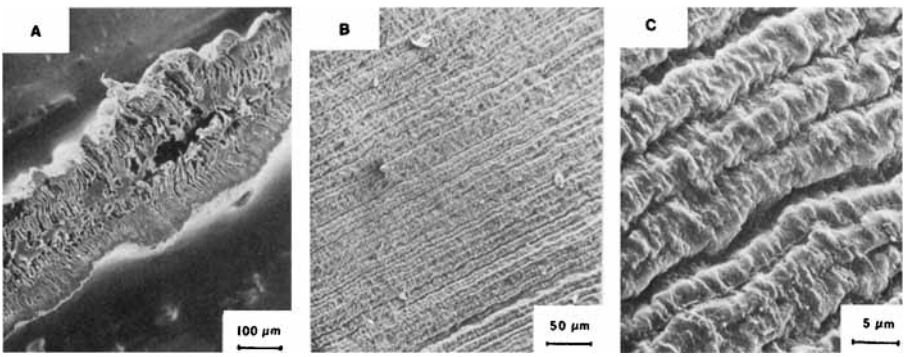

Fig. 11. SEM photomicrograph of extruded film: (A) cross section (50×); (B) surface (100×); (C) surface (1000×).

TABLE III
Biaxial Orientation Factors for Films

Run no.	Film process	f_{1c}^B	f_{2c}^B	f_{1b}^B	f_{2b}^B	f_{1a}^B	f_{2a}^B
1	Extruded	0.33	0.04	−0.19	−0.004	−0.18	−0.04
2	Extruded	0.22	0.04	−0.09	−0.02	−0.14	−0.03
3	Extruded	0.35	0.20	−0.15	−0.09	−0.20	−0.11
4	Extruded	0.30	0.16	−0.15	−0.08	−0.15	−0.08
5	Uniaxial drawdown	0.51	0.01	−0.23	−0.05	−0.28	−0.04
6	Uniaxial drawdown	0.52	0.21	−0.23	−0.10	−0.30	−0.11
7	Uniaxial drawdown	0.40	0.18	−0.17	−0.10	−0.23	−0.08
8	Uniaxial drawdown	0.46	0.18	−0.17	−0.06	−0.29	−0.11
9	Mandrel	0.21	0.17	−0.04	−0.03	−0.02	−0.14
10	Mandrel	0.16	0.25	−0.03	−0.04	−0.14	−0.21
11	Mandrel	0.23	0.27	−0.59	−0.07	−0.17	−0.20
12	Mandrel	0.35	0.45	−0.12	−0.14	−0.23	−0.31
13	Mandrel with drawdown	0.27	0.16	−0.07	−0.04	−0.27	−0.13

SEM Photomicrographs

SEM Photomicrographs of film cross sections are shown in Figures 11–13. The thick films with little drawdown exhibit complex void structures near the center of the film cross section. The voids are elongated and perpendicular to the machine direction. For the uniaxially drawdown films and those stretched over the mandrel, the voids show a much lower stage of development. The voids were not visible in SEM; the surface appeared to be solid. Biaxial films exhibited a solid cross section similar to the uniaxially drawn films.

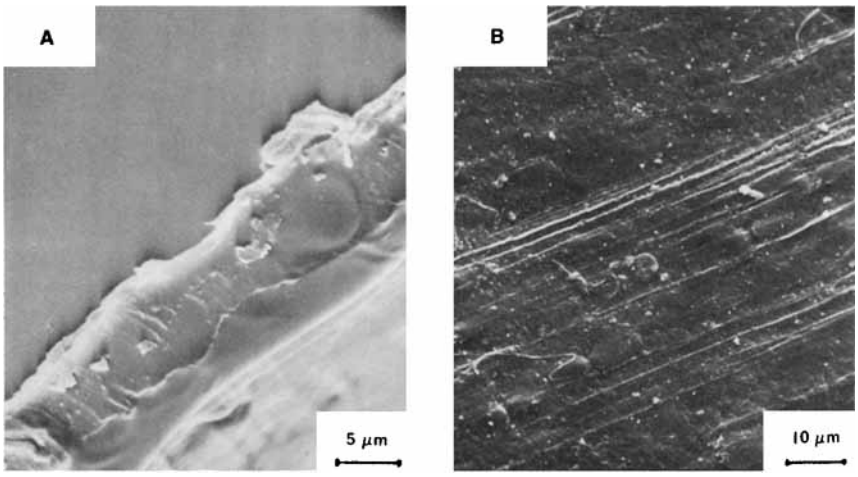

Fig. 12. SEM photomicrographs of uniaxial drawdown film: (A) cross section (1000×); (B) surface (500×).

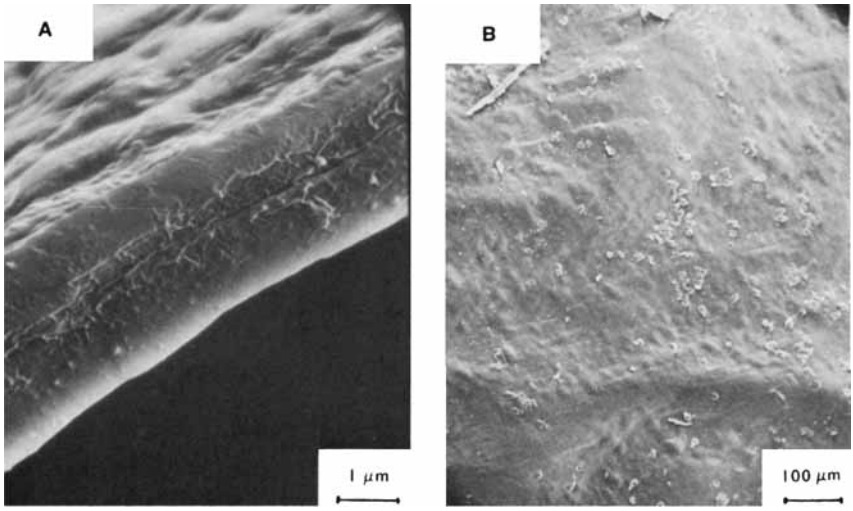

Fig. 13. SEM photomicrographs of film extruded over a mandrel: (A) cross section (5000×); (B) surface (50×).

Shrinkage

The percent shrinkages of the film after removal from the coagulant are summarized in Table IV. The shrinkage is primarily a function of the state of orientation and only secondarily related to coagulant. Other factors may also be involved.

TABLE IV
Shrinkage of PPD-T Films

Coagulant	Film process	Shrinkage (%) Machine direction	Shrinkage (%) Transverse direction
100% H_2O	Extruded	73	73
55% MeOH 45% H_2O	Extruded	5.4	38
75% MeOH 25% H_2O	Extruded	24	33
100% MeOH	Extruded	15	30
100% H_2O	Drawdown	0	20
55% MeOH 45% H_2O	Drawdown	1.3	17
75% MeOH 25% H_2O	Drawdown	0	28
100% MeOH	Drawdown	5.7	30
100% H_2O	Mandrel	—	—
55% MeOH 45% H_2O	Mandrel	—	—
75% MeOH 25% H_2O	Mandrel	2	0
100% MeOH	Mandrel	0	0

TABLE V
Mechanical Properties of PPD-T Films

Run no.	Film coagulant by volume	Film process	Modulus (Pa)			Tensile strength (Pa)		
			MD	45°	TD	MD	45°	TD
1	50% MeOH 50% EtOH	Extruded	1.1×10^9	2.4×10^8	5.1×10^8	2.9×10^7	7.6×10^6	1.4×10^7
2	55% MeOH 45% H_2O	Extruded	3.8×10^9	Broke in[a] clamp	Broke in[a] clamp	1.2×10^8	—	—
3	75% MeOH 25% H_2O	Extruded	2.1×10^8	1.4×10^8	6.9×10^7	3.1×10^6	2.1×10^6	1.4×10^6
4	100% H_2O	Extruded	1.4×10^9	1.1×10^8	1.2×10^8	9.0×10^7	3.1×10^7	6.2×10^6
5	50% MeOH 50% H_2O	Drawdown	3.0×10^9	1.1×10^9	6.2×10^8	1.2×10^8	2.3×10^7	6.7×10^7
6	55% MeOH 45% H_2O	Drawdown	6.1×10^9	9.0×10^7	9.6×10^7	1.5×10^8	6.6×10^6	9.0×10^6
7	75% MeOH 25% H_2O	Drawdown	3.2×10^9	2.9×10^8	8.3×10^7	1.2×10^8	7.6×10^6	7.6×10^6
8	100% H_2O	Drawdown	8.3×10^9	5.0×10^9	6.0×10^8	2.5×10^8	1.3×10^8	1.5×10^7
9	50% MeOH 50% EtOH	Mandrel	1.0×10^9	1.5×10^9	1.2×10^9	4.9×10^7	5.8×10^7	5.5×10^7
10	50% MeOH 50% EtOH	Mandrel	—	—	—	—	—	—
11	75% MeOH 25% H_2O	Mandrel	1.4×10^9	2.6×10^9	2.8×10^9	6.4×10^7	1.1×10^8	9.2×10^7
12	75% EtOH 25% H_2O	Mandrel	8.3×10^8	5.0×10^9	3.0×10^9	6.6×10^7	9.0×10^7	9.0×10^7
13	50% MeOH 50% EtOH	Mandrel with drawdown	2.0×10^9	6.8×10^8	6.8×10^8	9.7×10^7	2.3×10^7	2.7×10^7

[a] This sample was exceptionally smooth or wrinkle-free compared to the other samples. There were slight twists or contortions throughout the sample, though, which in combination with the routine brittleness contributed to the sample breaking upon being clamped.

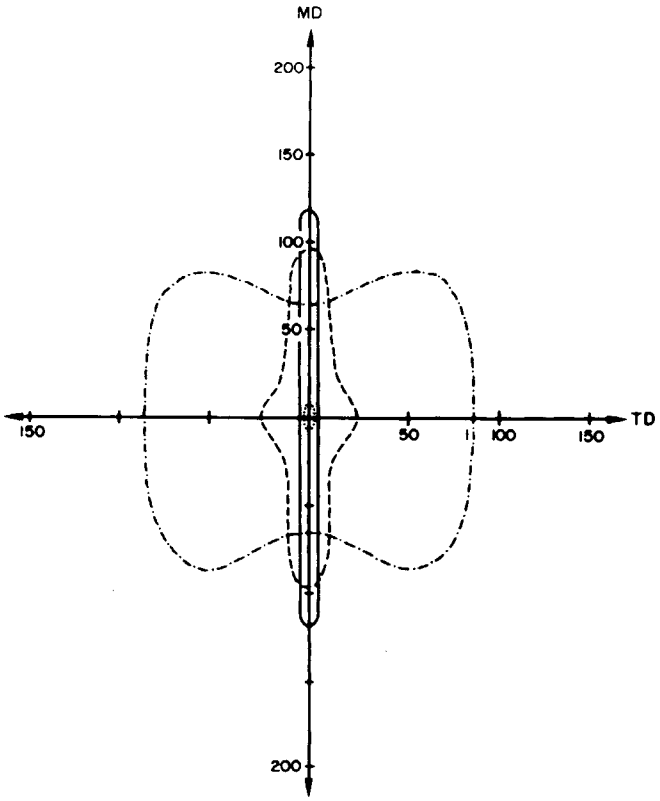

Fig. 14. Polar diagram of modulus as a function of direction in the PPD-T film ($\times 10^{-7}$ Pa): (·····) extruded only, run 3; (——) uniaxial drawdown, run 7; (-·-) mandrel, run 9; (- - -) mandrel with drawdown, run 13.

Mechanical Properties

Typical modulus and breaking stress data may be seen in Table V. The Young's modulus of the films are of order 2×10^8–8.3×10^9 Pa. Polar diagrams of the tensile strength of the PPD-T films are shown in Figure 14 and 15. It can be seen that the uniaxial films are highly anisotropic with tensile strength of order 1.2×10^8 Pa in the machine direction and 7.5×10^6 Pa in the transverse direction. Uniaxially drawn films coagulated in water had tensile strengths in the machine direction as high as 2.8×10^8 Pa. Films produced using a mandrel have more balanced mechanical behavior. Tensile strengths in the machine and transverse directions of 5.2×10^7 Pa are observed.

The elongations to break of the films are of order 3–16% for the simple extruded films in the machine direction and 3–12% in the transverse direction. For the uniaxial films, they are 3–12% in the machine direction and much smaller in the transverse direction. For the biaxial films, we obtain 7–11% in the machine and 4–8% in the transverse. Percent elongation was difficult to quantify in terms of film direction due to film wrinkling, especially for the undrawn films, and the uniaxially drawn film. Wrinkles were usually in the machine direction. Other problems with edge effects and voids probably contributed to premature failure in all of the films.

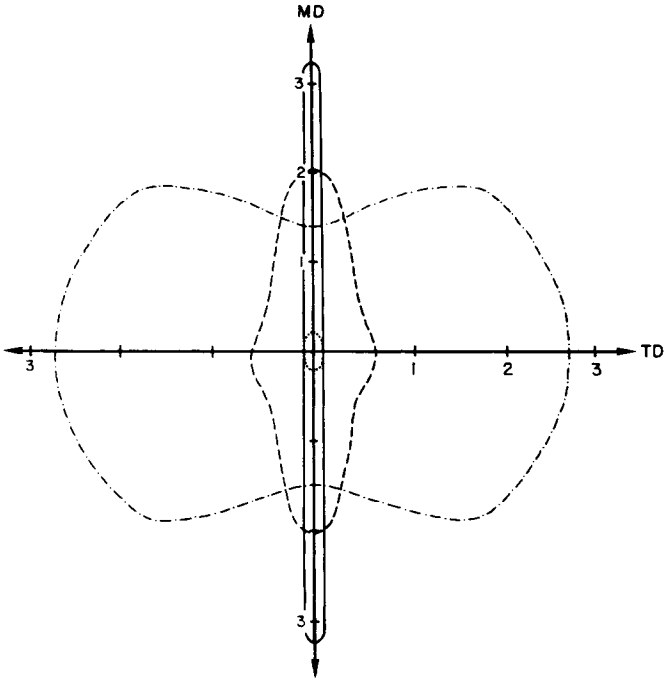

Fig. 15. Polar diagram of tensile strength as a function of direction in the PPD-T film ($\times 10^{-7}$ Pa): (·····) extruded only, run 3; (——) uniaxial drawdown, run 7; (-·-) mandrel, run 9; (- - -) mandrel with drawdown, run 13.

DISCUSSION

Crystallography

The films formed in the water coagulating baths exhibited different reflections from those formed in alcohol coagulants. Similar observations have been made on wet spun fibers by Hancock et al.[5] in our laboratories. Haraguchi, Kagiyama, and Takayanagi[49] have confirmed this and proposed that there is a second crystalline modification with a different unit cell. This has an orthorhombic form with dimensions a = 0.80 nm, b = 0.51 nm, and c = 1.29 nm (chain axis). Only the a and b crystallographic axis repeat distances change dimensions, as would be expected.

Orientation

There are some striking observations on the orientation development in the film process. First it is found that films extruded directly into the bath exhibited significant uniaxial orientation even though no tensions were applied. This orientation may be presented by the biaxial orientation factors.

The retention of flow orientation after exiting from the die is suggested by the observations of Onogi et al.[25] of a very slow birefringence decay in hydroxypropylcellulose solutions. Striking retention of die orientation in extruded filaments of liquid crystalline hydroxypropylcellulose melts was also reported by Shimamura et al.[16]

The second remarkable observation is the successful formation of an equally

biaxial oriented film with biaxial orientation factors as high as 0.35 and 0.45. Values of f_c^B and f_c^B of 0.5 represent an equal and complete biaxial planar orientation. While it has been established at least since the work of Blades[2] that it is possible to develop high levels of uniaxial orientations from liquid crystalline polymers, it has not been previously realized that one may obtain such levels of equal biaxial orientation.

Mechanical Properties

The variation in mechanical properties with film orientation indicated striking effects. While high machine direction modulus (8×10^9 Pa) may be developed in uniaxial films, they are brittle and fibrillate readily in the transverse direction. However, once equal biaxial orientation is achieved, good properties may be otained in all directions in the plane of the film. It should also be noted that none of these films have been annealed under tension as is the case of Kevlar® fibers. Annealing Kevlar® fibers under tension at temperatures of 300–500°C is known to create a marked increase in modulus and tensile strength.[2] Typical modulus, tensile strength, and per cent elongation values for Kevlar® fibers are, respectively, 8.3×10^{10} Pa, 3.6×10^9 Pa, and 4.4. Biaxially oriented poly(ethylene terephthalate) films have been reported[50] with property values of modulus, tensile strength, and per cent elongation being respectively 4×10^9 Pa, 2.5×10^8 Pa, and 1–4%.

FUTURE WORK

Much needs to be done to optimize the process described in this paper. We have not as yet carefully investigated the annealing of the films which will probably upgrade their properties. Annealing plays a key role inthe formation of high modulus aromatic fibers.[1,2,4] Also we have only looked at a single mandrel shape. By varying the cone-angle or even going to other mandrel shapes we may be able to produce films of quite different characteristics. We wish to scale up our process to higher production rates and enable not only longer runs but the formation of larger annular films.

This research was supported by the Office of Naval Research.

References

1. S. L. Kwolek, U.S. Pat. 3,671,542 (1972).
2. H. Blades, U.S. Pat. 3,767,756 (1973).
3. P. W. Morgan, *Macromolecules*, **10,** 1381 (1977).
4. S. L. Kwolek, P. W. Morgan, J. R. Schaefgen, and L. W. Gulrich, *Macromolecules*, **10,** 1390 (1977).
5. T. A. Hancock, J. E. Spruiell, and J. L. White, *J. Appl. Polym. Sci.*, **21,** 1227 (1977).
6. I. Hay, seminar, University of Tennessee, ca. 1975.
7. W. J. Jackson and H. F. Kuhfuss, *J. Polym. Sci., Polym. Phys.*, **14,** 2043 (1976); U.S. Pat. 3,778,410 (1973); U.S. Pat. 3,804,805 (1974)
8. W. J. Jackson, *Br. Polym. J.*, 154 (1980).
9. W. J. Jackson and H. F. Kuhfuss, *J. Appl. Polym. Sci.*, **25,** 1685 (1980).
10. J. J. Kleinschuster, U.S. Pat. 3,991,014 (1976).
11. G. W. Callandam, U.S. Pat. 4,067,852 (1978).
12. B. P. Griffin and M. K. Cox, *Br. Polym. J.*, 147 (1976).
13. J. I. Jin, S. Antour, C. Ober, and R. W. Lenz, *Br. Polym. J.*, 132 (1980).

14. R. S. Werbowj and D. G. Gray, *Mol. Liq. Cryst. Lett.*, **34,** 97 (1976); *Macromolecules*, **13,** 69 (1980).
15. M. Panar and O. B. Willcox, W. German Pat. 27 65 0382 (1977).
16. K. Shimamura, J. L. White, and J. F. Fellers, *J. Appl. Polym. Sci.*, **26,** 2165 (1981).
17. S. M. Aharoni, *Macromolecules*, **12,** 94 (1979).
18. C. P. Wong, H. Ohnuma, and G. C. Berry, *J. Polym. Sci., Polym. Symp.*, **65,** 173 (1978).
19. Y. Onogi, J. L. White, and J. F. Fellers, *J. Polym. Sci., Polym. Phys.*, **18,** 663 (1980).
20. J. Bheda, J. F. Fellers, and J. L. White, *Coll. Polym. Sci.*, **250,** 1335 (1980).
21. S. P. Papkov, V. G. Kulichikhin, V. D. Kalmykova, and A. Y. Malkin, *J. Polym. Sci., Polym. Phys.*, **12,** 753 (1974).
22. E. Iizuka, *Mol. Crystl. Liq. Cryst.*, **25,** 287 (1974).
23. H. Aoki, J. L. White, and J. F. Fellers, *J. Appl. Polym. Sci.*, **23,** 2293 (1979).
24. D. G. Baird, *J. Appl. Polym. Sci.*, **22,** 2701 (1978); *J. Rheol*, **24,** 465 (1980).
25. Y. Onogi, J. L. White, and J. F. Fellers, *J. Non Newt. Fluid Mech.*, **7,** 121 (1980).
26. J. Bheda, J. F. Fellers, and J. L. White, *J. Appl. Polym. Sci.*, **26,** 3955 (1981).
27. H. Aoki, Y. Onogi, J. L. White, and J. F. Fellers, *Polym. Eng. Sci.*, **20,** 221 (1980).
28. J. W. Hyatt, U.S. Pat. 204,228 (1878).
29. M. R. Gerow, U.S. Pat. 2,720,680 (1955).
30. M. T. Cichelli, U.S. Pat. 2,987,765 (1961).
31. M. R. Gerow, U.S. Pat. 3,084,386 (1963).
32. E. L. Fallwell, U.S. Pat. 3,092,874 (1963).
33. M. R. Gerow, U.S. Pat. 3,304,352 (1967).
34. F. A. Carlson, U.S. Pat. 3,619,445 (1971).
35. J. F. Flood, M.S. thesis, Polymer Engineering, University of Tennessee, 1982.
36. R. B. Bird, W. E. Stewart, and E. N. Lightfoot, *Transport Phenomena*, Wiley, New York, 1960.
37. J. R. A. Pearson and C. J. S. Petrie, *Plast. Polym.*, **38,** 85 (1970); *J. Fluid Mech.*, **40,** 1 (1970); *ibid*, **42,** 609 (1970).
38. K. J. Choi, J. L. White, and J. E. Spruiell, *J. Appl. Polym. Sci.*, **25,** 2777 (1980).
39. W. Flugge, *Stresses in Shells*, Springer-Verlag, Berlin, 1960.
40. R. A. Wessling, *Trans. Soc. Rheol.*, **9,** 95 (1965).
41. R. A. Wessling and T. Alfrey, *Trans. Soc. Rheol.*, **8,** 85 (1964).
42. P. A. Gutteridge, *J. Non Newt. Fluid Mech.*, **4,** 73 (1978).
43. T. Kaneda, S. Ishikawa, H. Daimon, T. Katsura, M. Ueda, K. Oda, and M. Horio, *Makromol. Chem.* to appear.
44. L. E. Alexander, *X-ray Diffraction Methods in Polymer Science*, Wiley, New York, 1969.
45. K. J. Choi, J. E. Spruiell, and J. L. White, *J. Polym. Sci., Polym. Phys.*, **20,** 27 (1982).
46. J. L. White and J. E. Spruiell, *Polym. Eng. Sci.*, **21,** 859 (1981).
47. M. G. Northolt, *Eur. Polym. J.*, **10,** 799 (1974).
48. R. S. Stein, *J. Polym. Sci.*, **31,** 327 (1958).
49. K. Haraguchi, T. Kajiyama, and M. Takayanagi, *J. Appl. Polym. Sci.*, **23,** 915 (1979).
50. K. Matsumoto, *Bull. Fac. Tax. Sci., Kyoto Univ. Tex. Fib.*, **7**(2), 279 (1974).

Received December 3, 1981
Accepted January 29, 1982